# Compositional mixture in R.F. sputtered CdTe oxide films. Raman spectroscopy results

F. Caballero-Briones and A. Zapata-Navarro.
*CICATA-IPN Unidad Altamira*
*Km 14.5 Carretera Tampico-Puerto Industrial Altamira, 89600 Altamira, Tamps., México.*

A. Martel and A. Iribarren
*Facultad de Física-IMRE Universidad de La Habana*
*Vedado 10400. La Habana, Cuba*

J. L. Peña, R. Castro-Rodríguez and P. Bartolo-Pérez
*Departamento de Física Aplicada, CINVESTAV-IPN Unidad Mérida*
*AP 73 Cordemex, 97310 Mérida, Yuc., México*

F. Rábago-Bernal
*Instituto de Física, Universidad Autónoma de San Luis Potosí*
*Av. Alvaro. Obregón 64, 78000, San Lus Potosí, SLP., México*

S. Jiménez-Sandoval
*CINVESTAV-IPN Unidad Querétaro*
*AP 1-798, 76001 Querétaro, Qro., México*

In this work, radiofrequency sputtered CdTe oxide (CdTeO) films with different oxygen contents were studied by Raman spectroscopy. In films with oxygen contents minor than 0.37 at., we observed bands associated with the LO and 2LO modes of CdTe. As oxygen content increases up to 0.60 at., they appear bands related with $[TeO_3]^{-2}$ trigonal pyramids and with $[TeO_4]^{-4}$ trigonal bipyramids, similar to those reported by other authors in metal-oxide doped $TeO_2$ glasses. Some additional peaks beyond 750 $cm^{-1}$, that we have related with $[CdO_6]^{-}$polyhedra and with $Cd_xTe_yO_z$ compounds, were observed in that films. We conclude that films evolve from crystalline CdTe to a glassy material where a mixture mainly composed of Te, Cd-Te, $[TeO_3]^{-2}$ and $[TeO_4]^{-4}$, structural units is formed as the oxygen content in the films increases from 0.15 at. to about 0.60 at. fraction.

*Keywords:* Glasses; Amorphous semiconductors-infrared and Raman spectra; Auger spectroscopy; Thin films growth; structure; and epitaxy
*PACS:* 61.43.Fs; 78.30.L; 82.80. P; 68.55

## 1. Introduction

Amorphous CdTe oxide (*a*-CdTeO) thin films have been studied in the last decade because of its potential applications in the optoelectronic and solar cell industries where they may play a role in the fabrication of CdTe-based devices, similar to that of amorphous $SiO_2$ in silicon-based devices [1]. The optical properties of *a*-CdTe:O films have shown that the optical energy gap can be tuned between 1.48 eV and 3.35 eV by controlling the oxygen content of the films [2].

CdTeO films are currently prepared by rf reactive sputtering, using an Ar-$N_2$ plasma, which is thought to catalyze the CdTe oxidation by the residual or added oxygen [1-3], or using a highly oxidizing gas such as $N_2O$ [4-6]. Within this method, amorphous films with oxygen contents between 0.07 and 0.60 at. are typically obtained with the substrate at room temperature. In post-annealed CdTeO films has been found evidence of crystalline phases such as $CdTeO_3$ and $CdTe_2O_5$; however, the structure of the as-deposited films has been difficult to elucidate.

In previous works [4,5] we had shown that the oxygen incorporation causes a change in the Te valence from $Te^{-2}$ to $Te^{+4}$. We proposed that the simultaneous presence of $Te^{-2}$ and $Te^{+4}$ causes a mixed compound structure in the middle-oxygen region, where the films will be composed by Cd-Te and $[TeO_4]^{-4}$ molecular subunits [6]. It was proposed that $[TeO_4]^{-4}$ subunit formation is aleatorious and causes the amorphization of the films [6].

Raman spectroscopy is a very sensitive technique to local order. It has been used to monitor the crystalline quality in II-VI semiconductors [7,8] and to study the structure of telluritic glasses ($TeO_2$) doped with different metal-oxides (MO) [9-13], but to the best of our knowledge, few Raman works are published in amorphous or microcrystalline films.

In the present work we study *a*-CdTeO films by Raman spectroscopy. The observed bands were related to those

*Corresponding author. E-mail fcaballero@ipn.mx, Tel & Fax 01 833 2600125*

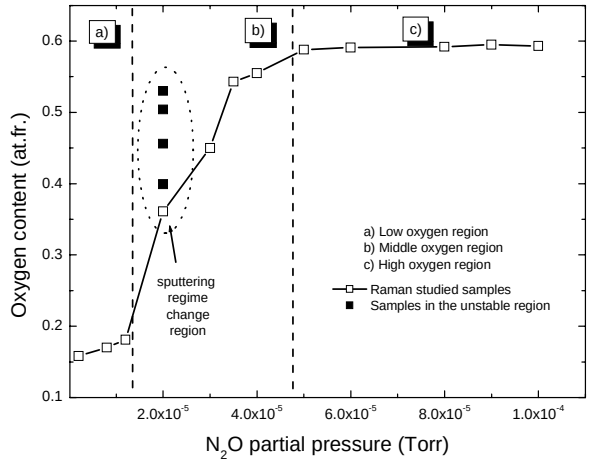


**Figure 1.** Oxygen contents in the films vs $N_2O$ partial pressures used

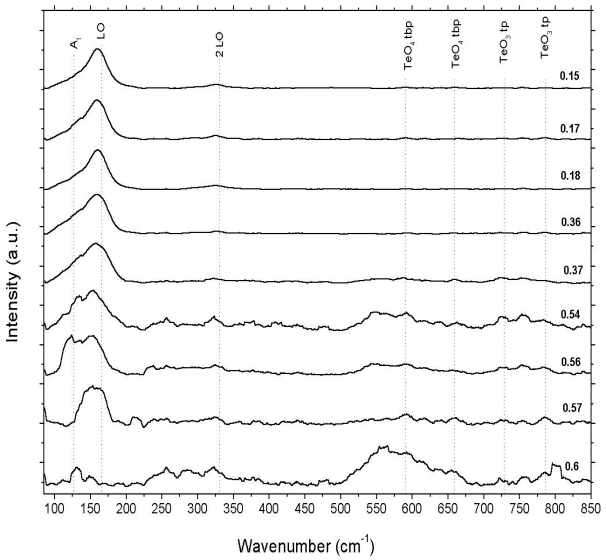


**Figure 2.** Normalized intensity Raman spectra of films with different oxygen content. The oxygen content is pointed at the right of each curve.

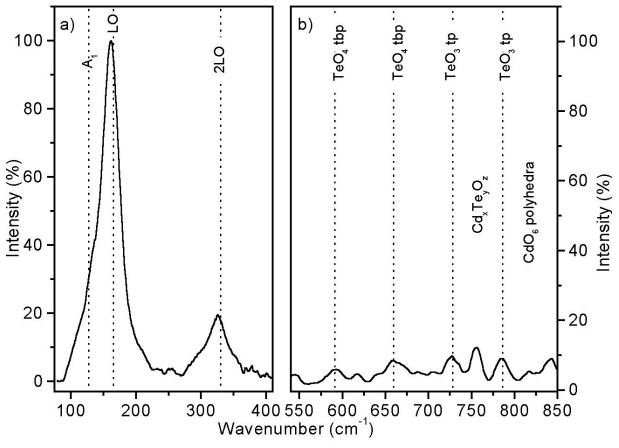


**Figure 3.** Typical Raman spectrum at low oxygen content. a) CdTe peak region. b) Glass peak region.

observed in CdTe and MO-doped $TeO_2$ glasses, and compared with our previous results.

## 2. Experimental procedures

The films were prepared in a CVE 301 (Cooke Vacuum Products) sputtering system with a US Gun II magnetron powered by a rf source from Advanced Energy Products. We used a 25 mm diameter CdTe target, pressed from 99.999% purity CdTe powder (Cerac). 99.999% purity Ar (Linde) and $N_2O$ (MG industries) were used as working gases. Films were deposited onto 12 x 12 mm, degreased and ultrasonically cleaned Corning glass slides. The substrate holder temperature was kept constant at 50º C. The deposition time was 15 minutes. The total working pressure was 2 x $10^{-2}$ Torr and the plasma power was 30 W. Films were growth at different $N_2O$ partial pressures, first introducing the $N_2O$ with a variable leak valve (Granville Phillips) to reach the desired $N_2O$ pressure as measured by a hot cathode vaccuometer (Granville Phillips) and then completing with Ar to the working pressure. Before the film deposition the target was Ar-presputtered for 5 minutes. The films were highly adherent, showing with increasing oxygen content, gradual colour change from gray to transparent. The obtained films present thicknesses between 0.8 and 1.5 μm. Thickness decreases when the partial pressure of $N_2O$ increases.

The oxygen content of the samples was determined by AES in an ESCA/SAM PHI 560 from Perkin Elmer, using the previously reported oxygen sensitivity factor [4]. Before analysis, the samples were eroded 1 min with a 2 keV $Ar^+$ beam.

The Raman measurements were carried out at room temperature in a Labram Dilor micro Raman system using a 632.8 nm He-Ne laser and a low-noise thermoelectrically cooled CCD detector. The laser spot diameter on the sample surface was 2 μm and neutral density filters were used to avoid sample changes produced by laser heating effects. Similar spectra were obtained through the entire surface of the sample.

## 3. Results and discussion

In the Figure 1 are shown the oxygen atomic fractions of the films obtained at the different $N_2O$ pressures used. Films with oxygen contents between 0.16 and 0.59 at. fr. were obtained, when increasing the $N_2O$ pressure. An important increase in the oxygen content is observed above 1 x $10^{-5}$ Torr, as the $Te^{-2}$ in CdTe changes its valence to $Te^{+4}$ [4-6]. The points inside the circled zone are samples grown at equal conditions, but having very different oxygen concentrations. This is due to the change in the sputtering regime in this region, where it is difficult to obtain controllable films [14]. At $N_2O$ pressures above this unstable region, the oxygen contents in the films increases smoothly, to finally reach values close to the stoichiometric saturation of CdTe i.e. 0.60 at. fr.. This behaviour defines roughly three regions, as seen in the Figure: the low, the

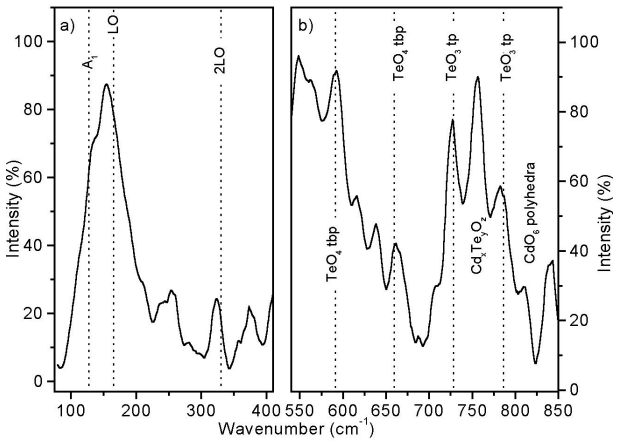


**Figure 4.** Typical Raman spectrum at middle oxygen content. a) CdTe peak region. b) Glass peak region.

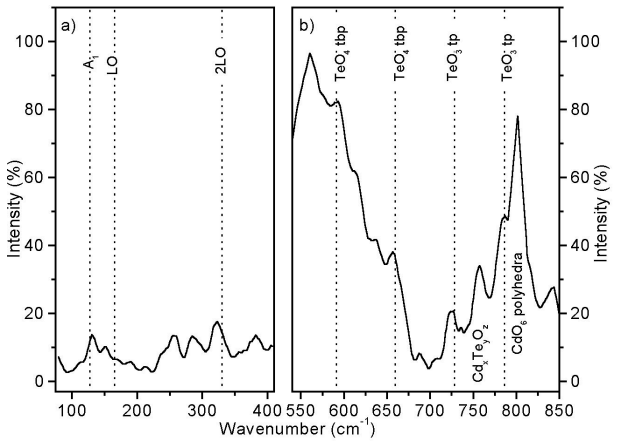


**Figure 5.** Typical Raman spectrum at high oxygen content: a) CdTe peak region. b) Glass peak region.

middle and the high oxygen regions, related to the amount of $Te^{+4}$ present in the films. A more detailed discussion of the oxygen incorporation mechanisms to CdTeO films will be subject of a future work.

The films were studied using Raman spectroscopy. The signal/noise ratio of the raw spectra falls at high wavenumbers when the oxygen content increases. Such behaviour can be related to the film composition evolution from CdTe-like compounds to Glass-like ones when the oxygen content increases. The background has a reverse behaviour, increasing at high wavenumbers when the oxygen content in the films increases. It is known [7] that the background is not a negligible part in the Raman scattering signal since it arises from multiple order scattering or fluorescence, and must be taken into account for quantitative measurements. Nevertheless, in the results described here, a qualitative description of the main features is considered sufficient.

The spectra shown in Figure 2 were background-subtracted by applying a polynomial function, and normalized to the maximum value. The oxygen atomic fraction of the films increases from the top to the bottom. The spectra will be analysed within two regions named in this work CdTe-like region, below 400 $cm^{-1}$ and Glass-like region, above this value. In the CdTe region are labelled three bands, related to CdTe and to hexagonal Te. In the Glass region we identified a set of bands related to tellurite glasses. For the assignment of the bands we used the values reported in refs. [8-13] as shown in Table I.

It is important to point out that the peak positions on the Raman bands in telluritic glasses move in relative wide limits depending on the cation type and its concentration [10,15]. Mean positions will appear in dotted line in all figures. We did not find evidence of $SiO_2$ related bands, indicating that films are thick enough to avoid glass substrate detection.

In Figure 2 it can be seen that the films with less than 0.37 oxygen content present well defined features related to the LO and 2LO bands of CdTe. The next samples, i.e. 0.54–0.57 O at. fr., show the above mentioned LO and 2LO CdTe bands and a band related with the Te $A_1$ mode. It also appears a wide band about 500-700 $cm^{-1}$ associated with $[TeO_4]^{-4}$ trigonal bipyramids (tbp) and a band between 700-800 $cm^{-1}$ related to $[TeO_3]^{-2}$ trigonal pyramids (tp). The last sample, with 0.59 O at.fr., shows very weak CdTe-related bands, a well-defined 500-700 $cm^{-1}$ band and a more deformed and lower intensity 700-800 $cm^{-1}$ band.

We do not observe bands around 450 $cm^{-1}$ in any sample, which have been related to bending vibrations of the Te-O-Te linkages in a continuous $TeO_2$ network [9-11].

The results indicate that a CdTe-related structure is present through almost the entire range of oxygen contents, being gradually substituted by an oxidized material that present bands closely related to those reported for tellurite glasses. The absence of the 450 $cm^{-1}$ band confirms that the $TeO_2$ continuous network of $[TeO_4]^{-4}$ tbp is not formed, as a high Cd concentration is always present [5], but a glassy mixture of Te, Cd-Te, $[TeO_3]^{-2}$ and $[TeO_4]^{-4}$ molecular subunits interlinked. CdTe in microcrystalline form can be assumed as the LO modes are clearly defined. The Te presence could be explained in terms of Te aggregates, frequently found in CdTe films, especially when growth on amorphous substrates [8]. The amount of such aggregates could be very small, but relative high-level signals are obtained due to the strong resonance in the Raman effect when Te crystals are excited by laser radiation of about 2 eV [16].

By the other hand, it is well known that the frequency and temperature factor of the intensity of a Raman Peak is given by the expression [17,18]:

$$R = cte\ \frac{[\upsilon_o + \upsilon]^4}{\upsilon}\ \frac{1}{1-\exp\left[-\frac{h\upsilon}{k\,T}\right]} \qquad (1)$$

where $\boldsymbol{\nu_o}$ and $\boldsymbol{\nu}$ are the frequencies of the exciting laser and the scattered light, respectively, k the Planck constant and T the sample temperature.

Following to other authors [12,19] we performed the

**Table 1.** Literature review of Raman band assignments for Te, CdTe and binary telluritic glasses [8-13].

| **Band** ID | **Wavenumber** ($cm^{-1}$) | **Vibration mode** |
|---|---|---|
| $A_1$ | 125 | Phonon vibrations -Te structure |
| LO | 165 | Phonon vibrations - CdTe structure |
| 2LO | 325 | Phonon vibrations - CdTe structure |
| A | 770-780 | Stretching vibrations-$TeO_3$ tp |
| B | 720-760 | Stretching vibrations -$TeO_3$ tp |
| C | 650-670 | Stretching vibrations - $TeO_4$ tbp |
| D | 600-615 | Stretching vibrations $TeO_4$ tbp |
| E | 400-500 | Bending vibrations -[Te-O-Te] or [O-Te-O] linkage |

temperature-frequency correction, i.e. after background subtraction; the spectrum is divided by the factor ***R***. The correction is a non-linear transformation of the spectrum, which will have the greatest effect in the lower-wavenumber portion of spectra. This region will be intensity-compressed and the positions of peaks will slightly move toward higher wavenumbers. The procedure is similar to the $k^2$-weighing performed to the EXAFS spectra to amplify the oscillations at high *k* [20].

Figure 3 shows the corrected Raman spectrum of the sample with 0.18 oxygen atomic fraction. This spectrum is typical of the low oxygen region: **a)** At wavenumbers <400 $cm^{-1}$, it can be seen well-defined LO and 2LO bands of CdTe at about 165 $cm^{-1}$ and 325 $cm^{-1}$ respectively. **b)** The region from 550 $cm^{-1}$ to 800 $cm^{-1}$ shows very weak, noisy bands. This result indicates that film consists basically of CdTe.

Figure 3 shows the corrected spectrum of the sample with 0.54 oxygen atomic fraction, which corresponds to the middle oxygen content region. **a)** Between 100-400 $cm^{-1}$ it can be noticed that the CdTe 2LO region is worse defined and weaker, suggesting a less ordered material. The Te $A_1$ peak can be distinguished here as a shoulder in the 100-200 $cm^{-1}$ region. **b)** The region >500 $cm^{-1}$ shows clearly defined $[TeO_4]^{-4}$ tbp bands, at about 590 and 660 $cm^{-1}$ and $[TeO_3]^{-2}$ tp bands at about 720, 780 $cm^{-1}$. Sekiya *et al.* [13] investigated the Raman spectra of $M_xTe_yO_z$ (M = Ba, Mg, Zn) crystals and found main peaks between 725 and 790 $cm^{-1}$ that they assigned these to the stretching vibration between Te and non-bridging oxygen atoms. Following Sekiya, the feature at about 750 $cm^{-1}$ could be related with $Cd_xTe_yO_z$ microcrystalline compounds [13]. Compared with the spectrum in Figure 3, it can be seen that the intensity of the bands in the Glass region is similar with the CdTe region. These results indicate that Cd-Te bonding is leading place to an aleatorious mixture of tellurium coordination states that are responsible for the loss of crystalline ordering of the films. The Figure also shows a feature at about 800 $cm^{-1}$ that can be related to Cd-O bonding which is analyzed below.

Figure 5 displays the corrected spectrum of the sample with 0.59 oxygen atomic fraction, near the stoichiometric saturation of CdTe, i.e. 0.60 at. fr., (all Te in $Te^{+4}$ state). The figure shows: **a**) a drastic reduction of the bands in the <400 $cm^{-1}$ region due to the global decreasing of the CdTe phase. A very doubtful evidence of Te $A_1$ band can be noted, indicating that Te-Te bonds are practically not present. **b**) The predominance of the Glass region bands is clear in this spectrum, as expected with the increasing of the Te-O bonding. Here, all the above-mentioned features, i.e. the $[TeO_4]^{-4}$ tbp, $[TeO_3]^{-2}$ tp, and $Cd_xTe_yO_z$ are present. The feature at about 800 $cm^{-1}$ is stronger and more defined than in the Figure 4. Duverger [11], who has investigated MgO-, PbO- and ZnO-doped $TeO_2$ glasses, has pointed out that it is essential to consider the contribution of the stretching vibration involving dopant metal and oxygen in the band upper 730 $cm^{-1}$. $[ZnO_6]^-$ polyhedra had been found by Kozhukharov *et al*. [21] in ZnO-doped $TeO_2$ glass. Then, the feature at about 800 $cm^{-1}$ could be related to O-Cd-O linkages in $[CdO_6]^-$ polyhedra.

In the Figure 5, the $[TeO_3]^{-2}$ bands seem to be relatively reduced compared with the Figure 4 spectrum and the $[TeO_{3+1}]$ seem to increase. This may be understood as a tendency of the material to form exclusively a $[TeO_4]^{-4}$ network, deformed by the Cd presence, however, in the present state of our study we cannot discriminate them by the observed Raman bands.

The above results are consistent with our previous results that show Te changes its valence from $Te^{-2}$ in CdTe to $Te^{+4}$ in $CdTeO_3$, with a mixture of them at the intermediate oxygen contents [4,5]. This change of valence will induce the aleatorious formation of the mentioned molecular subunits, as we have pointed out earlier [6], with the correspondent loss of ordering. Further work will be performed to quantify the amounts of the $[TeO_3]^{-2}$, $[TeO_4]^{-4}$ and $[TeO_{3+1}]$ molecular subunits with respect to the amount of oxygen present and to the Cd to Te bonding in order to get a more detailed description of the structure evolution of this material.

## 4. Conclusions

We study CdTeO films grown by reactive rf sputtering by Raman spectroscopy and found that they can be described as a mixture of structural subunits such as Cd-Te, $[TeO_3]^{-2}$, and $[TeO_4]^{-4}$. At low oxygen content CdTe is the dominant material. As Te changes its oxidation state from $Te^{-2}$ to $Te^{+4}$ with increasing oxygen content, $[TeO_3]^{-2}$ trigonal pyramids as well as $[TeO_4]^{-4}$ trigonal bipyramids are formed, and films tend to a glassy material. We found

some additional peaks beyond 750 $cm^{-1}$ that we related with $[CdO_6]^{-1}$ polyhedra and $Cd_xTe_yO_z$ microcrystalline compounds.

**Acknowledgements**

The authors would thank the support given to this work by W. Cauich for the AES measurements and F. Rodríguez-Melgarejo for the Raman measurements and to F. Chalé, P. Pasos, J. Zapata, M. Herrera, V. Rejón, O. Gómez and R. Sánchez for the technical support. We also thank the secretarial assistance by L. Pinelo. FCB and AZN acknowledge support to this work by CGPI-IPN and COFAA-IPN under EDI and SIBE grants. This work was partially supported by CONACYT under project number 38667-E.

**References**

[1] F.J. Espinoza-Beltrán, *et al.*, Jap. J. Appl. Phys. **30** 1715 (1991).
[2] F.J. Espinoza-Beltrán, R. Ramírez-Bon, F. Sánchez-Sinencio, O. Zelaya-Angel, G. Torres-Delgado, J.G. Mendoza-Alvarez, J. González-Hernández, M. H. Farías and L. Baños, Braz. J. Phys. **24** 426 (1994).
[3] M.Y. El Azhari, M. Azizan, A. Bennouna, A. Outzourhit, E.L. Ameziane and M. Brunel, Sol. Energy Mater. and Sol. Cells **45** 341 (1997).
[4] Zapata-Navarro, M. Zapata-Torres, V. Sosa, P. Bartolo-Pérez and J.L. Peña, J. Vac. Sci. Technol. A **12** 714 (1994).
[5] Zapata-Navarro, P. Bartolo-Pérez, M. Zapata-Torres, R. Castro-Rodríguez and J.L. Peña, J. Vac. Sci. Technol. A **15** 2537 (1997).
[6] Iribarren, E. Menéndez, R.Castro-Rodríguez, V. Sosa, J.L. Peña and F. Caballero-Briones, J. Appl. Phys. **86** 4688 (1999).
[7] Zwick and R. Charles, Phys. Rew. **48** 6020 (1994).
[8] S. Jiménez-Sandoval, S. López-López, B.S. Chao and M. Meléndez-Lira, Thin Solid Films **342** 1 (1999).
[9] V. R. Chowdari and P. Kumari, Mat. Res. Bull. **34** 327 (1999).
[10] H. Li, Y. Su, S. K. Sundaran, J. Non-Cryst. Solids **402,** 293 (2001).
[11] Duverger, M. Bouazaoui and S. Turrell, J. Non-Cryst. Solids **220** 169 (1997).
[12] Y. Himei, A. Osaka, T. Nanba and Y. Miura, J. Non-Cryst. Solids **177** 164 (1994).
[13] T. Sekiya, N. Mochida and A. Ohtsuka, J. Non-Cryst. Solids **168**, 106 (1994).
[14] M. Yoshitake, T. Yotsuya, S. Ogawa, Japn. J. Appl. Phys. **31**, 4002 (1992)
[15] H. Munemura, K. Mitone, M. Misawa, K. Nayurama, J. Non-Cryst. Solids **700** 293 (2001).
[16] P. M. Amirtharaj and F. H. Pollak, Appl. Phys. Lett. **45** (1984) 402.
[17] W. Kiefer "Raman Spektroskopie". Chapter 5 in "Spectroskopie amorpher und kristaliner Festköper". Eds. D. Haarer and W. Spiess, 115 (1995).
[18] "Vibrational Intensities in Infrared and Raman Spectroscopy". Eds. W. B. Person and G. Zerbi. Elsevier Sciantific Publishing Cpmpany. Amsderdam. (1982).
[19] B. Mysen, L. W. Finger, D. Virgo and F. A. Seifer. Am. Mineral **67** 686 (1982).
[20] M. Newville, "Fundamentals of EXAFS", Consortium of Advanced Radiation Sources, University of Chicago, 19 (2002).
[21] V. Kozhukharov, H. Burger, S. Neov, B. Sidzhimov. Polyhedron, **5** 771 (1986).